Microwave-assisted synthesis of carbon nanotubes for the removal of toxic cationic dyes from textile wastewater

Sundus Saeed Qureshi[1], Vaishali Shah[2], Sabzoi Nizamuddin[3], N.M. Mubarak[4*], Rama Rao Karri[4*], Mohammad Hadi Dehghani[5*], S. Ramesh [6,7], Mohammad Khalid[8], Muhammad Ekhlasur Rahman[9]

[1]Institute of Environmental Engineering and Management, Mehran University of Engineering and Technology, Jamshoro 76090, Sindh, Pakistan

[2]Department of Chemical and Petroleum Engineering, Faculty of Engineering, UCSI University, Kuala Lumpur-56000, Malaysia

[3]School of Engineering, RMIT University, Melbourne 3000, Australia

[4]Petroluem and Chemical Engineering, Faculty of Engineering, University of Technology Brunei, Bandar Seri Begawan BE1410, Brunei Darussalam

[5]Department of Environmental Health Engineering, School of Public Health, Tehran, University of Medical Sciences, Tehran, Iran.

[6]Center of Advanced Manufacturing and Material Processing, Department of Mechanical Engineering, Faculty of Engineering, University of Malaya, 50603, Kuala Lumpur, Malaysia

[7]Mechanical Engineering Programme Area, Faculty of Engineering, Universiti Teknologi Brunei, Tungku Highway, BE1410, Brunei Darussalam

[8]Graphene & Advanced 2D Materials Research Group (GAMRG), School of Engineering and Technology, Sunway University, No. 5, Jalan University, Bandar Sunway, 47500, Subang Jaya, Selangor, Malaysia

[9]Department of Mechanical & Construction Engineering at Northumbria University, Newcastle upon Tyne, United Kingdom

***Corresponding author (s):**
E-mail addresses: mubarak.yaseen@gmail.com; kramarao.iitd@gmail.com and hdehghani@tums.ac.ir

Abstract

Toxic cationic dyes are used in different textile industries. When the colour interacts with the sunlight, it causes incomplete photosynthesis, inhibiting aquatic organisms' growth and disrupting gas permeability in the water system. In this work, carbon nanotubes (CNTs) were

prepared to employ acetylene and hydrogen as precursor gases in a microwave-assisted reactor. The obtained CNTs were tested for their ability to remove the crystal violet (CV) dye. However, the effect of removal parameters, such as pH of ion solution, initial concentration, and contact time, was optimized on the adsorption process through response surface methodology. It was found that the optimized removal of CV dye was 81% at an optimum pH value of 7.0 with 10 mg/L of an initial concentration and a contact time of 25 min. Complete dye extraction can be achieved by increasing the CNT dosage. Moreover, by using both the Langmuir model and Freundlich model of adsorption, the equilibrium data obtained from experiments were analyzed. The study also revealed that the adsorption at room temperature having a high adsorption capability of 2.615 mg/g for CV was best defined using the Langmuir model. For the reaction order, the adsorption rates represented the pseudo-first-order kinetic model.

***Keywords**:* Adsorption; textile wastewater; carbon nanotubes; crystal violet; column studies

1. Introduction

Water is essential in life for various practices such as agriculture, industrialization, and ecological changes that alter the state of water resources, resulting in water contamination [1,2]. Water contamination is primarily caused by wastewater streams from industries that release contaminated effluents. It is essential to separate these pollutants before discharging wastewater into the environment. Textiles, plastics, paper, pharmaceuticals, photographic, pulp mills, paint, food, printing, leather, and cosmetics are the industries' that need many dyes to colour their products [3-5]. Many inorganic, organic, and biological pollutants have been found as water contaminants, including dyes, pesticides, fertilizers, microbes, and heavy metals, representing significant dangers. However, a smaller number is deemed carcinogenic [6-11].

Various types of dyes, such as natural, synthetic, and food dyes, are used in different industries [12,13]. Natural dye is extracted from vegetables, fruits, and flowers, an age-old practice since 3500BC to colour fabrics [14]. Synthetic dyes are categorized based on the chemical structure of

their specific chromophore group. Among different synthetic dyes, Azo dyes are the most fascinating and efficient dyes that have been recently utilized up to 90% in dyeing systems due to their versatility and ease of synthesis [15,16]. Various synthetic dyes are aromatic chemicals in nature. Some exceptions are classed as anionic, non-ionic (oil soluble), or cationic [4,17-19]. Methyl violet is a common cationic dye, whereas Azo dyes are anionic [20-22]. Synthetic dyes were widely employed in the textile and printing ink industries. The textiles industry, in particular generates the most water pollutants due to the residual dyes present in the wastewater after fabic processing. According to the World Bank, coloration and treatment of materials contribute to 17–20% of overall industrial water contamination. The water discharged while dyeing fabrics can remain visible for an extended period due to its resistance to biodegradation.

The dye waste has a high content of biological oxygen demand (BOD), which is undesirable for the surroundings. Dye contamination in wastewater causes several problems. One such issue is that the colour interacts with the sunlight, causing incomplete photosynthesis, thereby preventing the aquatic organism's growth and disturbing the solubility of a gas in the water [23]. Crystal violet (CV) is a cationic dye, also known as gentian violet, that can induce dermatitis, allergic reactions, restlessness, hyperactivity, cancer, mutation, and attention issues in humans. The characteristics features of this dye are primarily employed in veterinary and animal medicine and are a handy source in textile industries and as a biological staining process. Naturally, it is a carcinogenic compound and inadequately metabolized by microorganisms, non-biodegradable.

Various techniques for removing heavy metals and dyes from wastewater are available, including photocatalytic degradation, coagulation, liquid-liquid extraction, solvent extraction, reverse osmosis, oxidation, chemical precipitation, electrochemical treatment, adsorption, and membrane filtration. Many of these methods have drawbacks such as toxic sludge generation and waste products that must be disposed of safely, fouling, membrane scaling and blocking, and other disadvantages include high capital cost, incomplete metal removal, high energy

requirements, expensive equipment requirements, high operational costs, high reagent, and monitoring system requirements [24]. However, adsorption is regarded as the most effective of all the technologies listed as it provides adaptability in design and operation [25]. Furthermore, it is reversible, as suitable desorption processes can regenerate adsorbents for multiple uses [26].

Many adsorbents have been employed for dye removal from aqueous solution, including processed ginger waste, NaOH-modified rice husk, powdered bark of coniferous pines, teak, bottom ash, and polyaniline/hollow manganese ferrite nanocomposites, cupuassu shell, jujuba seeds, Brazilian pine fruit shell, chitosan, algae, inorganic silicates, activated carbon, carbon nanotubes coir pith, parthenium, coconut shell, and peanut hulls [27,28].

Microwave-assisted synthesis of carbon nanotubes (CNTs) is considered a simple, economical, rapid, clean, non-invasive, and environmentally friendly method [22,29-31]. Microwave irradiation accelerates the reaction at targeted areas by uniform and rapid heating thus improving the yield and characteristics of the main product. In addition to that, microwave irradiation promotes the functionalization and removal of certain existing functional groups in the treatment environment [32]. The CNTs are synthesized by microwave irradiation, which results in amorphous nanoporous surfaces with a high surface area that can potentially be employed as an adsorbent, allowing the adsorbent dosage to be reduced. Being an adsorbent, CNTs have attracted much interest amongst researchers since they offer an appealing option for removing organic and inorganic pollutants from water [33,34]. CNTs are utilized in the adsorption process because of their unique qualities, including chemical, physical, electrical, mechanical, and structural capabilities, extremely high thermal conductivity, optoelectronic, large specific surface area, and semiconductor [35].

This work investigates microwave-assisted CNTs for CV removal from aqueous solutions employing a batch column method. The effect of process parameters such as contact time, dye

solution pH, and initial concentration of dye removal efficiency were examined. In addition, the kinetic and isotherm studies for the adsorption of CV dyes were evaluated and explained.

2. Materials and Methods

2.1 Raw Materials

The dye utilized in this study was a crystal violet acquired from Merck. 1.0M sodium hydroxide and 1.0M hydrochloric acid were used to modify the pH of the stock solutions.

2.2 Synthesis of CNTs

Microwave-assisted carbon nanotubes were created following the principles established in our earlier research [36]. Using a microwave model Synotherm-T1500, China reactor, a ferrocene catalyst was inserted through the chamber entrance, while a quartz boat size of 50 mm ID, 55 mm OD, and 615 mm length was put in the middle of the reaction tube. Argon gas was used for flushing out the oxygen from the chamber. The C_2H_2 and H_2 gases were then combined (in a 0.6 ratio) and, employing a gas mixture apparatus (KM-20-2), circulated into the tubular microwave chamber. The reaction was carried out at 900 W reaction power and 35 min of radiation time.

2.3 Stock solution preparation

CV stock solutions with an initial concentration of 1000 mg/L were prepared for the adsorption investigation. The dye powder (1 g) and distilled water (1 L) were mixed and swirled to ensure a homogenous solution. Based on the experimental matrix produced from the Design-Expert version 11 (trial version), the dye solution was prepared with varied starting concentrations (2–10 mg/L) and varying pH (4–10) values.

2.4 Batch column adsorption experiments

The experimental setup used in this study for removing CV from the aqueous solution is shown in ***Figure 1***. Small-scale column tests were carried out to calculate the removal capacity

for removing CV from an aqueous solution. A plastic tube of 2.5 cm diameter and 5 cm height was used to conduct the adsorption tests at room temperature. The column was packed with the carbon nanotube at a certain height. The CV concentration was measured in the UV spectrophotometer.

100 mL sample of 10 mg/L CV solution was used for the batch adsorption experiment. All studies were performed at standard temperature-pressure (STP) conditions with a 1 g of adsorbent dose. 1.0 M of hydrochloric acid or 1.0 M of sodium hydroxide were used to adjust the pH of the dye stock solutions, depending on the desired pH value. The adsorption capacity was determined at the time (t) using Equation (1). The equilibrium of dye adsorption was calculated using Equation (2).

$$q_t = \frac{(C_o - C_t)V}{m}[(C_o - C_t)\,V]/m \quad (1)$$

$$q_e = \frac{(C_o - C_t)V}{m}[(C_o - C_e)\,V]/m \quad (2)$$

Where C_o is the initial concentration of dye solution (mg/L), C_t is the concentration of dye solution at time t (mg/L), C_e is the concentration of dye solution at equilibrium, m is the weight of carbon nanotube adsorbent employed (g), and V is the dye solution volume (L).

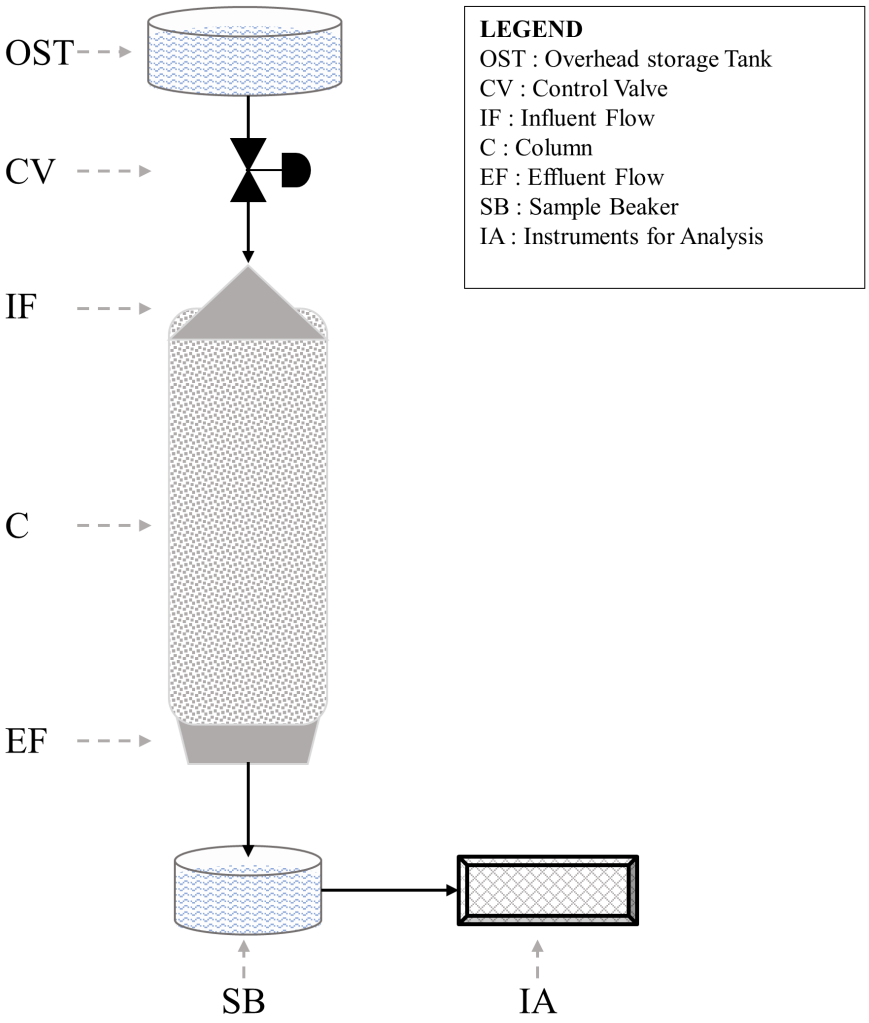

Figure 1: *Column studies experimental set-up for removal of the CV*

2.5 Characterization of CNTs

The CNTs were examined using a Philips XL30 scanning electron microscope (SEM). The imaging was performed in high vacuum mode at an operating voltage of 15kV, a spot size of 4.5-5, and a working distance of 10 mm. Moreover, the Fourier transform infrared (FTIR) spectroscopy was performed using a Perkin Elmer FTIR Spectrometer (TA 8000), with 32 scans per sample were recorded from 4000-550 cm^{-1} at a resolution of 4 cm^{-1}.

2.6 Isotherm and Kinetic studies conducted on CV adsorption using CNTs

The equilibrium data obtained from the experiments were fitted to different isotherm models to understand the inherent mechanisms in the CV adsorption process. The conventional

157 solid-liquid adsorption isotherm models (single component) evaluated in this study are
158 presented in **Table 1**. This table shows non-linear forms of isotherm models. It is a common
159 practice by most researchers to linearize the non-linear model expressions, as it is not
160 straightforward to calculate constants in the non-linear models. Even though the linearized
161 model equation adequately fits the equilibrium data, providing higher R^2, the predicted values
162 gave low values after the isotherm parameters were substituted in the non-linear model form.

163 Similarly, to understand the kinetic of the CV adsorption onto CNT, the experimental
164 values were validated with four prominent non-linear kinetic models, shown in **Table 1**. Also,
165 the parameters in these kinetic models were evaluated by linearizing the non-linear model
166 expressions. However, linearizing the non-linear models would depict wrong interpretation and
167 undervalues the kinetic models.

168 Further, to statistically validate the performance of predicted values with the
169 experiments, various prominent statistical (error) functions were chosen, as shown in **Table 2**.
170 These metrics confirm and validate the suitability of respective non-linear isotherm models and
171 evaluated parameters. For instance, if the metrics result in a smaller value (with the exception
172 of R^2) this means that the model-predicted values are in close agreement with the experimental
173 values; however, they vary distinctly if it produces a higher metrics results.

174 **Table 1:** *Different prominent isotherm and kinetic models (along with a number of parameters*
175 *they have in respective models) that were investigated in CV removal using CNT's*

Isotherm & Kinetic Models	Non-Linear Equations	Number of parameters
Isotherm Models		
Linear (Henry's Law) model	$q_e = KC_e$	1
Langmuir model	$q_e = \left(\frac{K_L b C_e}{1+bC_e}\right)$	2
Freundlich model	$q_e = K_F C_e^{1/n}$	2

Redlich-Peterson model	$q_e = \left(\frac{K_R C_e}{1 + a_R C_e^{\alpha}}\right)$	3
Sips model	$q_e = \left(\frac{K_S b C_e^{1/n}}{1 + b C_e^{1/n}}\right)$	3
Toth model	$q_e = \frac{K_{th} C_e}{\left(b^{'} + C_e^{\ n}\right)^{1/n}}$	3
Kinetic Models		
Pseudo 1st order	$q = q_e(1 - e^{-k_1 t})$	2
Pseudo 2nd order	$q = \left(\frac{K_2 q_e^2}{1 + t K_2 q_e}\right) t$	2
Weber - Morris model	$q = k_{id}\sqrt{t}$	1
Boyd model	$\frac{q}{q_e} = 1 - \frac{6}{\pi^2} exp(-Bt)$ $B = \frac{\pi^2 D_i}{r^2}$	2

176

177 **Table 2:** *Different prominent statistical (error) functions evaluated in this study*

Statistical (Error) functions
Coefficient of correlation $(R^2) = \frac{\sum_{i=1}^{n}\left[\left(q_{e,pred}^{i} - q_{e,exp}^{i}\right)^2\right]}{\sum_{i=1}^{n}\left[\left(q_{e,pred}^{i} - \bar{q}_{e,exp}^{i}\right)^2\right]}$
Sum of absolute error $(SSE) = \sum_{i=1}^{n}\left(q_{e,pred}^{i} - q_{e,\exp}^{i}\right)$
Pearson's Chi-square measure $(\chi^2) = \sum_{i=1}^{n}\frac{(q_{e,\,pred}^{i} - q_{e,\exp}^{i})^2}{q_{e,\,pred}^{i}}$
Root mean square error $(RMSE) = \sqrt{\frac{1}{n-1}\sum_{i=1}^{n}(q_{e,\,pred}^{i} - q_{e,\exp}^{i})^2}$
Hybrid fraction error function $(HYBRID) = \frac{100}{(p-n)}\sum_{i=1}^{p}\frac{(q_{e,\,pred}^{i} - q_{e,\exp}^{i})^2}{(q_{e,pred}^{i})^2}$

Where 'n' is the number of experimental runs and 'p' is the number of parameters; $q_{e,exp}^{i}$ is q_e (mg/L) experiment value for each run; $q_{e,pred}^{i}$ is q_e (mg/L) predicted (calculated) value for each run and $\overline{q}_{e,exp}^{i}$ is mean of all $q_{e,exp}$ (mg/L) values.

3. Results and Discussion

3.1 Statistical analysis for the removal of the CV

Design-Expert 11 (trail version) software was used to analyze the percentage removal of dye from pre-prepared stock solutions. The experimental matrix with factors (actual & coded) and crystal violet removal percentage using CNTs is given in ***Table 3***. The highest percentage removal was 85% for a pH value of 4.0, an initial concentration of 10 mg/L, and a contact time of 10 min. The lowest value observed is 40% at a pH of 4.0, an initial concentration of 2 mg/L, and a contact time of 10 min. The quadratic regression model equation is found using the variance analysis (ANOVA) summarized in ***Table 4***. The Fisher (F) value is used to demonstrate the model's efficiency. As the F-value increases, so does the model's efficiency. The F value was obtained by the regression mean square (MSR) ratio and mean square of the error (MSE). Freedom of 1 for pure error ensures that the lack of fit test was valid. The lower the probability (p) value, the more significant the model. It can be observed from ***Table 4*** that the p-value for the removal of crystal violet was <0.0001; this implies that the model is significant. The R-squared and Adj R-squared values were critical in determining the importance of a model. The R-squared and Adj R-squared values for removing CV were 0.98 and 0.97, respectively.

The developed equation for removing CV from the prepared stock solution using CNTs is shown in Equation (3).

$$\text{Removal \%} = 52.324 - 12.602 * A + 2.424 * B + 2.209 * C - 0.344 * AB - 0.0306 * AC - 0.0354 * BC + 1.187 * A^2 + 0.388 * B^2 - 0.0347 * C^2 \quad (3)$$

Whereas A represents the bar-coded value for the pH of the stock solution, B represents the rate of concentration, and C represents the duration of contact value, respectively. The above

equation represents the coded factors that may be utilized to interpret the different results of each element. For the positive values, these factors are represented by default as +1, while for the negative values, the factors are depicted as -1, respectively. Hence, the given equation is handy for determining relative elemental significance by contrasting the factors of the coefficients. The positive sign denotes that the parameters work together, whereas the negative sign represents resistance to the parameters.

Table 3:. *Experimental matrix with factors (actual & coded) along with crystal violet removal percentage using CNTs*

Run	Factor 1 A: pH	Factor 2 B: Concentration (mg/L)	Factor 3 C: Contact Time (min)	Response (% Removal)
1	10 (+1)	10 (+1)	40 (+1)	81
2	7 (+0)	6 (+0)	40 (+1)	52
3	4 (+-1)	2 (+-1)	40 (+1)	51
4	10 (+1)	10 (+1)	10 (+-1)	84
5	4 (+-1)	10 (+1)	40 (+1)	83
6	**7 (+0)**	**10 (+1)**	**25 (+0)**	**81**
7	10 (+1)	2 (-1)	40 (+1)	61
8	10 (+1)	2 (-1)	10 (-1)	60
9	10 (+1)	6 (+0)	25 (+0)	75
10	7 (+0)	6 (+0)	25 (+0)	58
11	7 (+0)	2 (-1)	25 (+0)	51
12	4 (-1)	6 (+0)	25 (+0)	66
13	7 (+0)	6 (+0)	10 (-1)	52
14	7 (+0)	6 (+0)	25 (+0)	58
15	4 (-1)	2 (-1)	10 (-1)	40
16	4 (-1)	10 (+1)	10 (-1)	85

Table 4: *ANOVA for removal of crystal violet using CNTs*

Source	Sum of Squares	df	Mean Square	F-value	p-value Prob > F	
Model	3173.07	9	352.56	113.24	< 0.0001	significant
A-pH	129.60	1	129.60	41.63	0.0007	
B-Concentration (mg/L)	2280.10	1	2280.10	732.36	< 0.0001	
C-Contact time (min)	4.90	1	4.90	1.57	0.2563	

AB	136.13	1	136.13	43.72	0.0006
AC	15.13	1	15.13	4.86	0.0697
BC	36.13	1	36.13	11.60	0.0144
A^2	301.25	1	301.25	96.76	< 0.0001
B^2	101.00	1	101.00	32.44	0.0013
C^2	160.82	1	160.82	51.66	0.0004
Residual	18.68	6	3.11		
Lack of Fit	18.68	5	3.74		
Pure Error	0.0000	1	0.0000		
Cor Total	3191.75	15			

3.2 The effect of process parameters on CV removal percentage

The influence of pH, contact time, and initial CV concentration on the CV removal percentage was investigated. The effect of pH was studied to determine the best pH where it exhibits the highest removal percentage. The pH was controlled by adding hydrochloric acid or sodium hydroxide to the stock solution. The pH values were adjusted using the pH meter model (Eutech Instruments). The pH is an essential factor for the uptake of CV because the medium pH influences the magnitude of the electrostatic charges imparted by the ionized dye molecules. The CV solution's initial concentration, adsorbent dosage, and temperature were 10 mg/L, 1.0 g/L, and 25 °C, respectively. The effect of pH ranges from 2 to 10 on CV dye removal by adsorption is shown in ***Figure 2 (a).*** Adsorption of dye increased with increasing pH. As the pH increased, H^+ ions decreased, making the process more favourable. Lower adsorption of CV at acidic pH was probably due to an excess of H^+ ions competing with the dye anions for the adsorption sites [37]. An increase in pH causes a decrease in the surface charge density. This lowers the electrostatic repulsion between the surface of the CNTs and the charge of CV. As a result, the rate of adsorption rises [38].

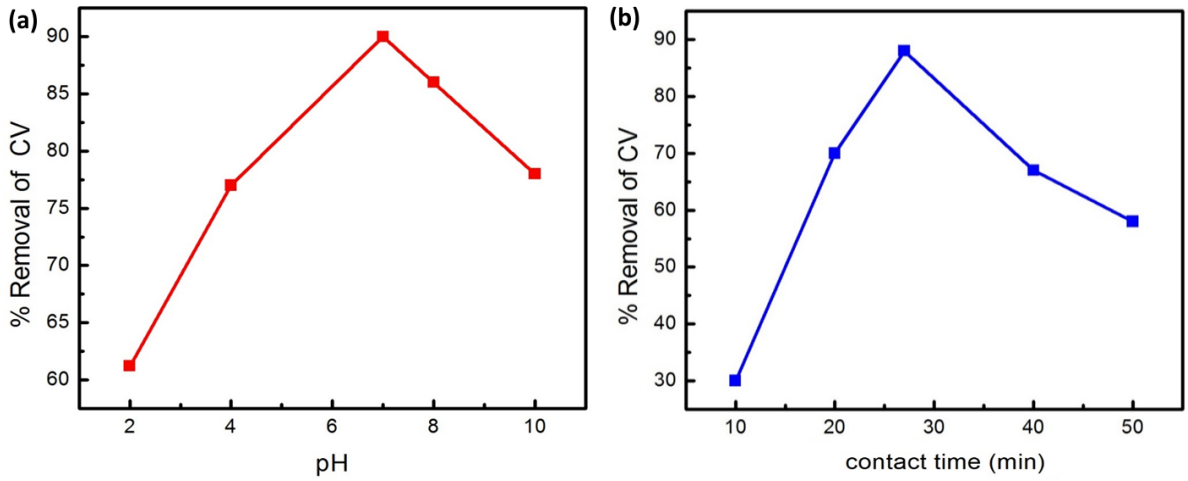

Figure **2:** ***Effect of different a) pH values*** *(b) contact times on CV removal*

With the initial concentration of 10 mg/L by utilizing CV solutions, different experiments were employed to optimize the adsorption time of dye. This study used a wide range of contact times, such as 10, 20, 30, 40, and 50 mins, to determine the removal efficiency. As shown in ***Figure 2 (b)***, the percentage removal of CV increased in the first 10 min until the equilibrium reached 30 min approximately, and it started decreasing after the equilibrium point (i.e., 30 min). At the initial stages, the acceleration of adsorption rate is facilitated due to the presence of a positively charged adsorbent surface for the transfer of anionic species present in the reaction solution. A decline in CV removal after the equilibrium point could be attributed to the fact that the remaining surface spaces were not occupied due to the dye molecules' strong repulsive interactions at the adsorbent surfaces and in the bulk solution [39]. It is reported that a rapid increase at the initial adsorption period is because the adsorbent surface performs fast initially and starts blocking adsorption sites indicating a gradual decrease in adsorption rate. However, a reduction in adsorption rate (after achieving equilibrium) is explained by phenomena explaining that adsorption sites are initially active. However, they get occupied gradually with time, leading to blockage of adsorption sites and a significant decrease of free sites, decreasing the adsorption rate [40]. The outcome obtained in this study about the effect of time on adsorption rate is in

agreement with previous studies recommending similar behaviour of adsorption rate with time [41-43].

The effect of the initial CV concentration was investigated while all other parameters remained constant. It was found that the removal percentage was more significant at lower initial concentrations of CV and vice versa. It was noted that 82% removal of CV was observed at 2 mg/L of initial concentration of CV, but it decreased to 49% at 10 mg/L of initial concentration of CV. The relative availability of adsorption sites can explain a higher CV removal percentage at 2 mg/L of initial concentration of CV and a lower CV removal percentage at 10 mg/L of initial concentration. The amount of dye molecules was less for 2 mg/L of CV solution, whereas the lower adsorption was due to an increase in the amount of dye molecules for the 10 mg/L. A decrease in the removal of CV at a higher initial concentration of CV is mainly due to the saturation of adsorbent sites at the surface of the adsorbent [44]. The removal percentage of CV was compared with the literature, as shown in **Table 5**. Similar results for higher CV removal at a lower initial concentration of CV and lower CV removal at a higher initial concentration of CV were reported in the literature [45] . A similar interaction mechanism as previously reported in the literature between CNTs and CV was observed in this study, thus suggesting that when the CV dye is adsorbed on CNTs, OH- from glycerol reacts with CNTs forming C-O-C-H bonds [34]. Based on a recent literature, Abbas et al. [46] proposed the rate of adsorption at four stages: (1) transfer of pollutants from the outer surface to the inner surface (rapid process), (2) displacement of pollutants once it reaches with an adsorbent surface (fast process), (3) diffusion of pollutants into the adsorbent surface under the action of initial concentration (prolonged process), and (4) adsorption of pollutant towards micropore (very fast process).

Table 5: Comparison of % CV removal observed this study with the relevant literature

Material	pH	Concentration (mg/L)	Contact time (min)	CV Removal (%)	Reference
CNT	4	10	10	85.0	This study
MWCNT	3-8	25-48	30-45	31	[47]
CNT	2-10	-	10-180	85	[34]
Titanate nanotube	6.8	20	120	80	[48]
Pumice	6.5	30	120	86.7	[49]
Formosa papaya seed powder	2-8	10-40	60	41.0	[50]
Grapefruit peel	1-10	10-600	30-240	96.1	[51]
Apple stem	10	100	20	96%	[52]
Date palm leaves	10	16.35	21.10	99.5%	[53]
mango leaves biochar	8	2500	48	99.85%	[54]
titanate nanotube	6.8	20	-	75%	[48]

The interaction between three parameters (pH, contact duration, and CV initial concentration) on the overall CV removal efficiency by CNT is shown in ***Figure 3***. Three different concentrations for the investigation were used with three different pH values, 4, 7, and 10, respectively. The initial concentration was increased from 2 mg/L to 10 mg/L; the lower concentration showed a lower removal rate at any value of pH and contact time. When the initial concentration was increased to 6 mg/L, the rate mechanism improved at any pH value. The optimum condition for the high removal rate was a pH of 10 and a residence time of 25 min at 10 mg/L; after that, the removal rate decreased**.** From this study, the optimal parameter values for CV removal are a pH value of 7.0, a contact time of 25 min, and an initial concentration of 10 mg/L, 81% of CV removal using CNT.

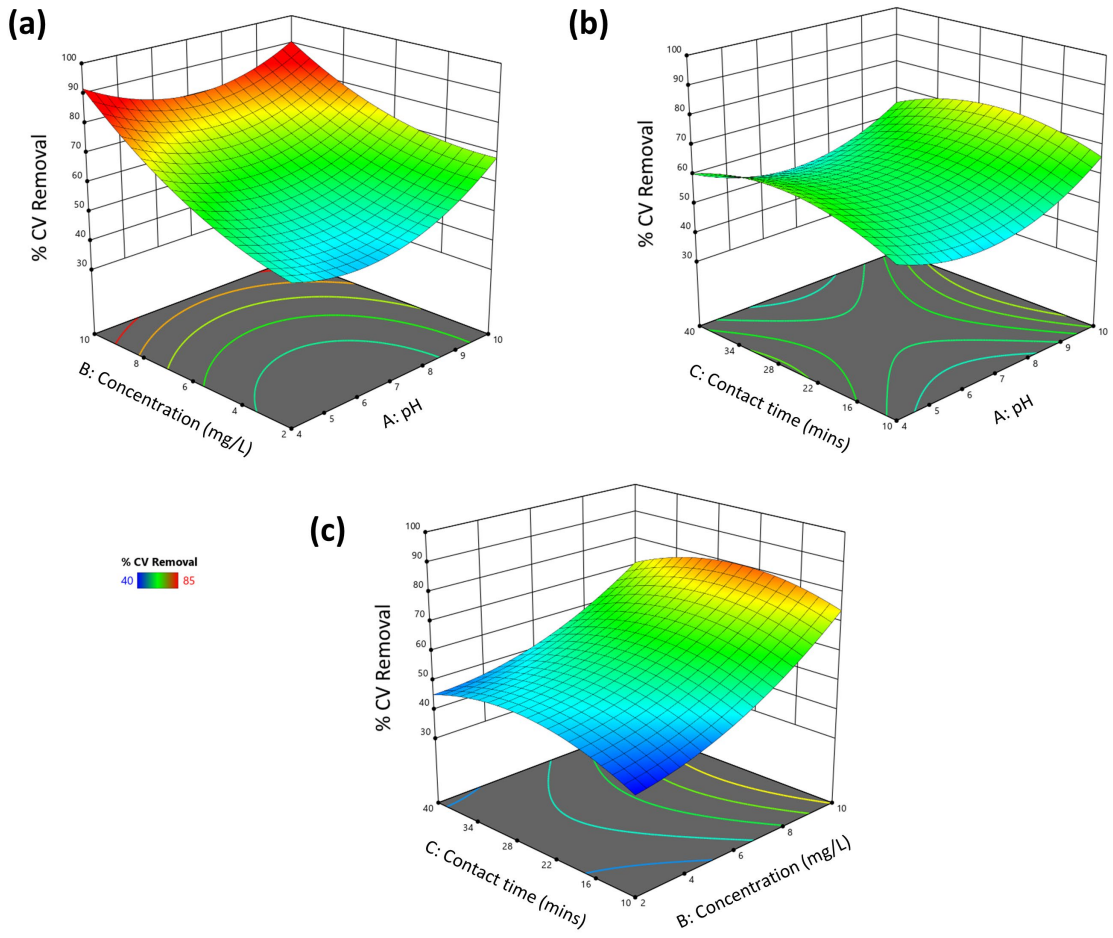

Figure 3: *Interaction of various parameters a) pH, b) Contact time (min), and c) Initial concentration (mg/L) on the overall CV removal*

3.3 CV adsorption kinetic studies

The study of kinetics is important in determining the chemical process rate. The kinetic study experiments lasted up to 40 min, with three distinct pH values and initial concentrations of dye solution. The solutions volume was kept constant at 100 mL, while the mass of the adsorbent was maintained at 1g. A UV-Vis Spectrophotometer was used to assess the concentration of the dye solution every 5 min.

It was found (***Figure 4***) that the CV removal from the stock solution increases with the contact time. ***Figure 4*** **(a)** shows the influence of pH values, with pH 10 removing the most within a contact time of 25 minutes. Similarly, ***Figure 4*** **(b)** represented the initial concentrations adsorption capacities against the contact time as observed. The initial concentration of 10 mg/L

showed the highest adsorption rate in contrast to other concentrations factors. The feedstock, which had the maximum initial concentration, showed the maximum removal efficiency over adsorbent CNTs compared to different initial feedstock concentrations. It showed that the increase in dyes' anion influenced the removal rate. The active dye site leads to the maximum active site and removes maximum CV anions.

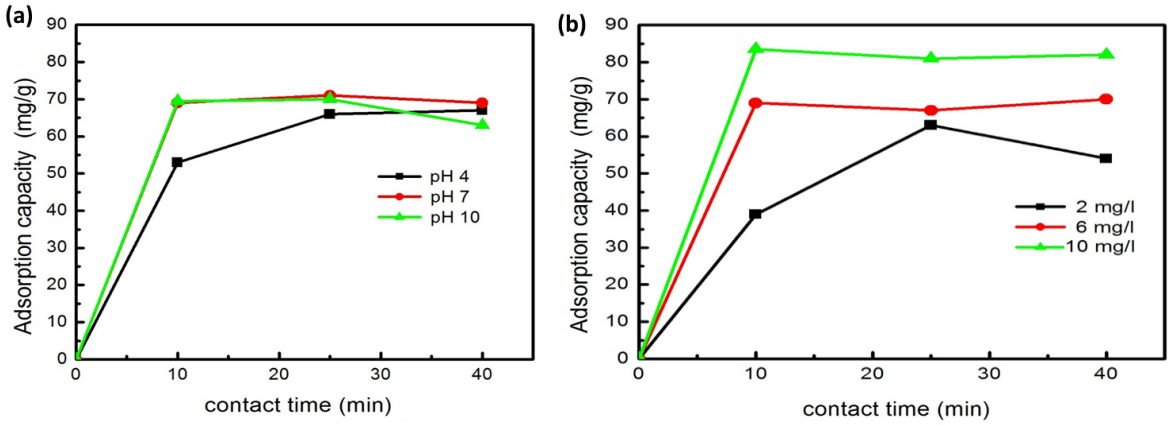

Figure 4: *Kinetic studies of crystal violet a) pH b) initial concentration*

To understand the adsorption mechanism of CV onto CNT, the equilibrium data was ~~is~~ validated with four isotherm models for each pH value. As mentioned earlier, the parameters in each isotherm model were evaluated using the non-linear approach. The fit of the isotherm model was ~~is~~ validated by computing various statistical metrics, as shown in ***Table 6***. These metrics confirm the fitness of the non-linear model. For pH 4, besides R^2 being high, all other statistical metrics are lower, thus ensuring pseudo-first-order (PFO) suitability. A similar trend was ~~is~~ observed for different pH values. Therefore, the kinetic parameters thus evaluated from non-linear expression are more reliable and correctly depict the inherent mechanisms. The comparative plots of fitting different kinetic models for different pH values are shown in ***Figure 5***. It can be noticed from these plots that, except for the Weber & Moris model, the remaining three kinetic models are in close agreement with the experimental values. However, PFO kinetic model is more suitable among these models. As previously stated, pH rises, enhances crystal violet removal, and has higher q_e values.

315 **Table 6:** *Comparison of various kinetic parameters along with different statistical metrics*

Statistical Metrics		PFO	PSO	Weber & Morris	Boyd
		Non-Linear	**Non-Linear**	**Non-Linear**	**Non-Linear**
Kinetic Parameters	pH 4	K_1: 0.175 q_e: 6.725	K_2: 0.033 q_e: 7.49	K_{id}: 1.228	B: 0.25 q_e: 6.7
	pH 7	K_1: 0.25 q_e: 6.858	K_2: 0.105 q_e: 7.144	K_{id}: 1.301	B: 0.292 q_e: 7.0
	pH 10	K_1: 0.229 q_e: 7.198	K_2: 0.462 q_e: 7.233	K_{id}: 1.375	B: 0.933 q_e: 6.8
Correlation coefficient of determination (R^2)	pH 4	0.9888	0.9996	0.9077	0.9856
	pH 7	0.9879	0.9979	0.8355	0.9992
	pH 10	0.9882	0.9946	0.7728	0.9942
Average relative error (ARE)	pH 4	3.6791	1.5610	24.0842	9.4707
	pH 7	3.0208	0.2599	29.1451	2.4980
	pH 10	7.8074	4.8995	35.9026	6.4748
Sum of the squares of errors (SSE)	pH 4	0.0881	0.0153	3.2747	0.7593
	pH 7	0.1076	0.0005	6.6293	0.0603
	pH 10	0.4286	0.2076	10.3869	0.5227
Sum of the absolute errors (SAE)	pH 4	0.4198	0.1964	2.8424	1.0385
	pH 7	0.3857	0.0352	3.8094	0.3218
	pH 10	1.1069	0.7049	5.0233	0.9506
Root-mean-square error (RMSE)	pH 4	0.2098	0.0875	1.2796	0.6162
	pH 7	0.2319	0.0160	1.8206	0.1737
	pH 10	0.4629	0.3222	2.2789	0.5112
Marquardt's percentage std dev (MPSD)	pH 4	4.0138	1.5493	23.9879	11.9928
	pH 7	10.3200	14.5573	24.9267	17.8246
	pH 10	19.1860	25.8304	28.2291	21.0955
Pearson's Chi-square measure	pH 4	0.9924	0.9988	0.7105	0.9404
	pH 7	0.9538	0.9147	0.7314	0.8786
	pH 10	0.8572	0.7736	0.7093	0.8414
Hybrid fractional error (HYBRID)	pH 4	0.1790	0.0267	6.3935	1.5981
	pH 7	1.1834	2.3546	6.9038	3.5302
	pH 10	4.0900	7.4134	8.8542	4.9447

316

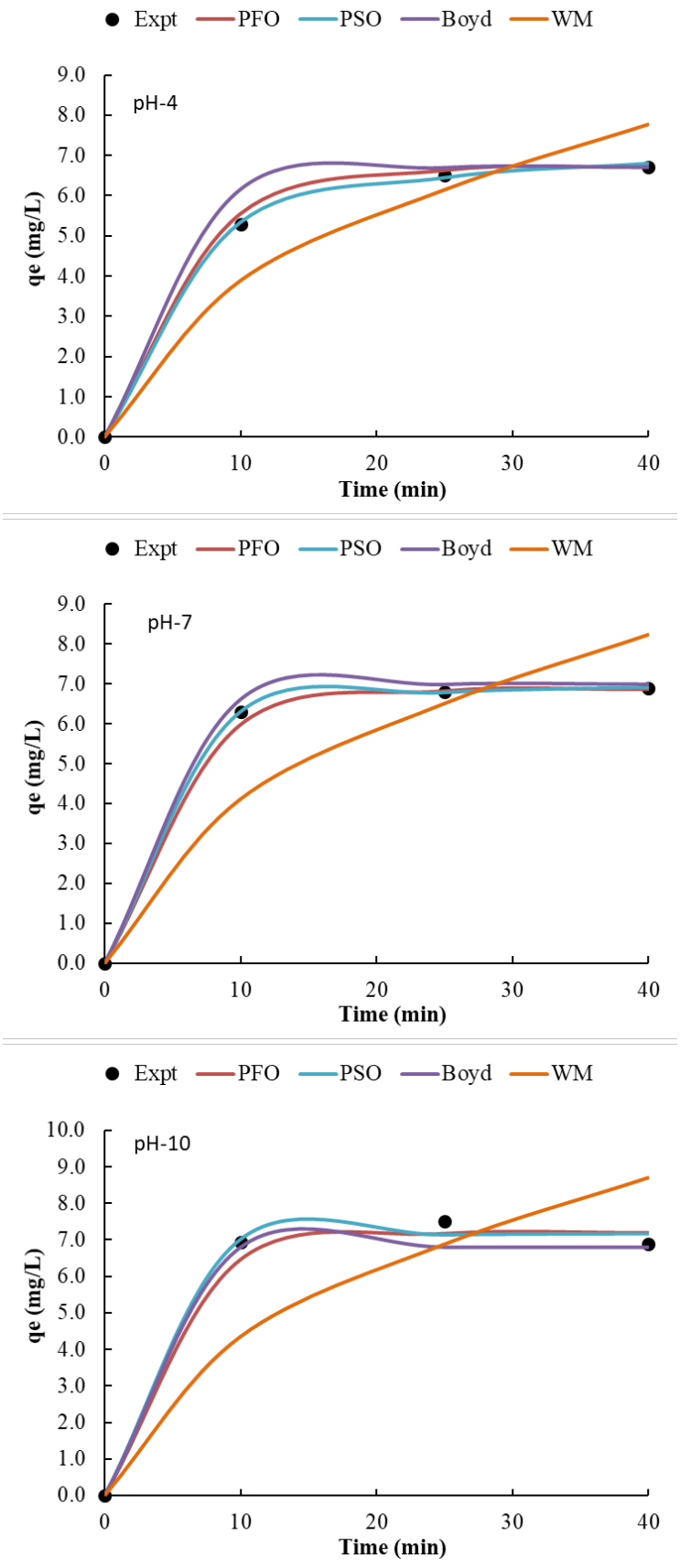

317

318 **Figure 5:** *Comparison of different kinetic models for pH values of 4, 7 and 10*

The experimental kinetics of CV adsorption on CNT observed a rapid increase in adsorbed concentration during the first 1–2 min, followed by a slower absorption rate, as suggested by the Weber & Morris model. The initial part is accompanied by faster mass exchange through the limit layer and adsorption on the solid surface, followed by moderate dispersion within the particles. Hence, both the intra-particle and mass transfer rates are governed as the rate-limiting steps in this step. The transport rate is affected by the solid's structure and its interaction with the dispersing agent. The adsorbent might be permeable impediments and solute development by dispersion from one liquid body to the other via the concentration slope. In Intra-particle diffusion, the species move from the bulk of the solution towards the solid phase. This model was proposed to anticipate the process of adsorption rate occurring on a porous adsorbent surface in a well-stirred batch adsorption process.

3.4 CV adsorption isotherm studies

The adsorption isotherm tests used three different initial concentrations to remove crystal violet. Three volumetric flasks of 100 mL were employed, each with a dye solution of 2 mg/L, 6 mg/L, and 10 mg/L, respectively. Adsorbent dosage, pH, and temperature variables were kept constant at 1g of CNTs, pH value of 6.0, and room temperature.

These adsorption studies are verified against 6 prominent isotherm models. As stated earlier, most researchers linearize the non-linear model expressions. Even though the linearized model equation adequately fits the equilibrium data, providing higher R^2, the predicted values give low values after the isotherm parameters are substituted in the non-linear model form. Hence non-linear analysis is used to evaluate the model parameters without linearizing the non-linear expressions. The comparison of various isotherm parameters and different statistical metrics is given in **Table 7**. Among the validated isotherm models, Langmuir isotherm models seem to be more appropriate, resulting in an R^2 value of 0.998. Besides the highest R^2, all other statistical metrics resulted in lower values. The amount of q_m was observed to be 2.615 mg/g, and the K_L

344 value was noted to be 8.034 L/mg. The comparison of the performance of different isotherm
345 models investigated in this study is shown in **Figure 6**. The best fitting of Langmuir and
346 Freundlich isotherm models suggests that they can be used to estimate the adsorption of CV dye
347 from an aqueous solution using carbon nanotubes.

348 **Table 7:** *Comparison of various isotherm parameters along with different statistical metrics*

Nonlinear models	Parameters	R^2	SSE	RMSE	χ^2	HYBRID
Henry (Linear) model	K: 13.73	0.9788	0.0142	0.0596	0.0456	-19.1389
Langmuir model	KL: 8.034 qmax: 2.615	0.9979	0.0005	0.0027	0.0001	-0.9566
Freundlich model	KF: 7.021 n: 1.311	0.9883	0.0010	0.0155	0.0020	-0.3548
Redlich-Peterson model	aRP: 6.178 KRP: 22.621 g: 0.875	0.9849	0.0033	0.0287	0.0037	11.4289
SIPS model	Ks: 8.117 qms: 2.787 ns: 0.999	0.9855	0.0079	0.0443	0.0093	19.8341
TOTH model	aT: 0.165 KT: 2.772 nT: 0.908	0.9839	0.0063	0.0396	0.0089	-22.7050

349

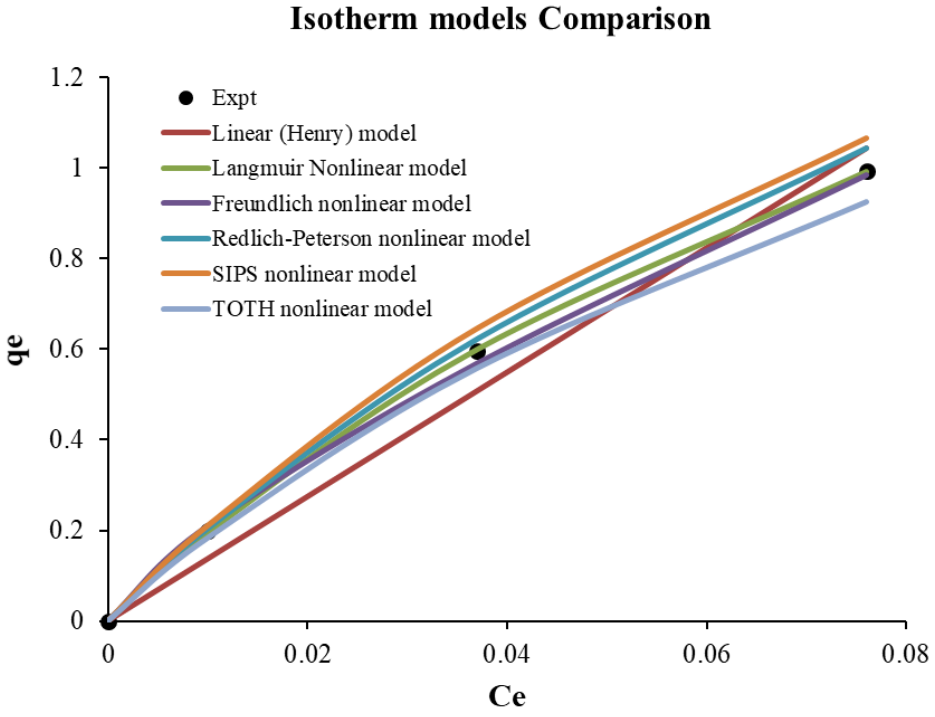

350

351 **Figure 6:** *Comparison of performance of fitting different isotherm models*

352 *3.7 Characterization of CNTs before and after adsorption*

353 The CNTs used in this study were characterized through SEM analysis and FTIR analysis
354 before and after the adsorption of CV dye. The SEM images of CNTs before and after adsorption
355 of CV dye are shown in ***Figure 7***. The surface texture of the raw CNTs (before adsorption) is
356 smooth, and there are only a few pores visible on the surface, as seen in ***Figure 7* (*a*)**. On the
357 other hand, the CNTs, after being used for the adsorption of CV dye (see ***Figure 7* (*b*)**), showed
358 that the tubes opened up, resulting in a less smooth surface when compared to the raw CNTs,
359 possibly due to the attachment of some functional groups during adsorption.

360

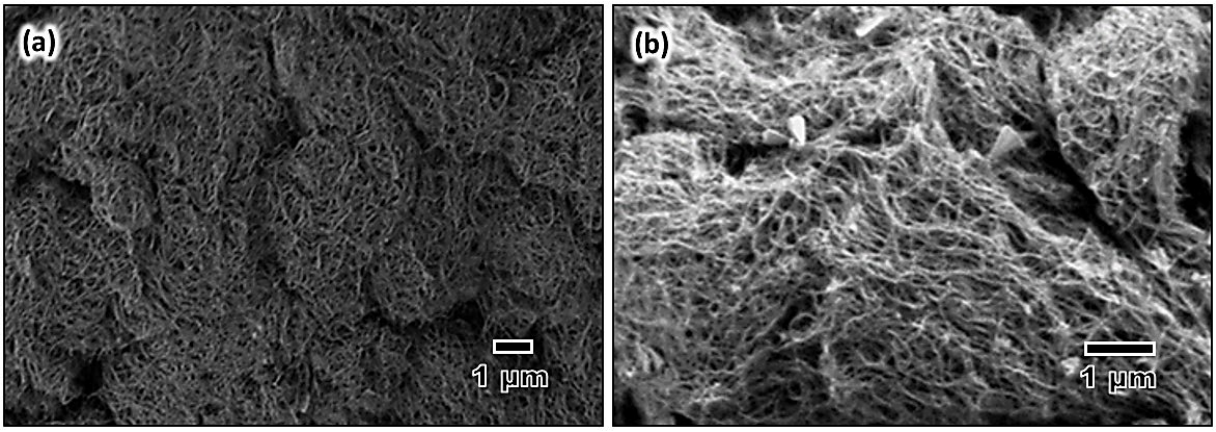

361
362 **Figure 7:** *SEM images of CNT (a) before adsorption and (b) after adsorption of CV dye*

363 The chemical reactivity on the adsorbent surface, noticeably in the form of chemisorbed
364 oxygen in the different functional groups, is an essential factor that regulates the function of
365 CNT. The FTIR spectra, before and after CV dye adsorption is shown in ***Figure 8***. The results
366 show that the functional groups appeared on the adsorbent's surface following adsorption. The
367 peak seen at approximately 3500 cm^{-1} for CNTs before adsorption, demonstrating the present
368 of hydrogen-bonded O–H stretching on the CNT's surface. After adsorption, a broad peak
369 appears on the functional group side of the O–H bond due to the water adsorption on the CV.
370 C–H stretching vibrations resulting from the adsorbent causes a strong peak to appear between
371 2850-3000 cm^{-1}. A sharp peak of C = O stretching vibration at approximately 1600–1750 cm^{-1}

resembles the carbonyl groups in the CNTs, e.g., carboxylic acid, ketones, and aldehydes. C = C stretching vibrations occur at approximately 1650 cm^{-1} due to an aromatic compound, e.g., benzene. Furthermore, the C–H bending vibration at 1150 cm^{-1} indicates the presence of an alkane group and this was confirmed by the presences of a strong absorption peak at about 700–610 cm^{-1}.

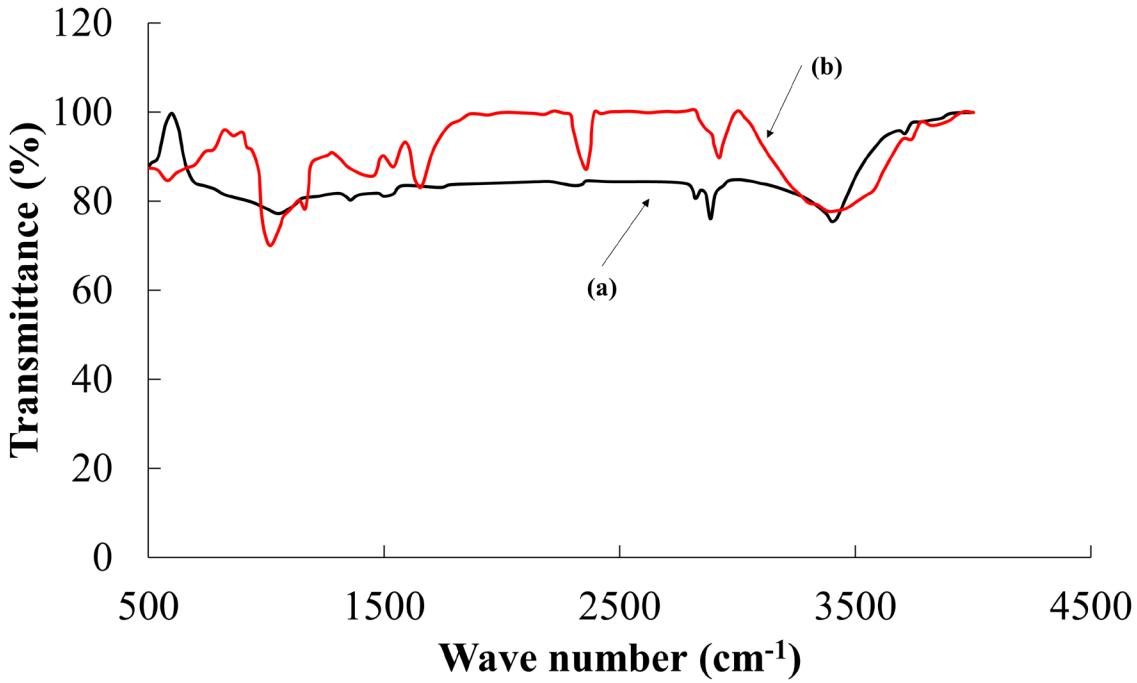

Figure 8: *FTIR analysis of CNTs (a) before adsorption and (b) after adsorption*

8. Conclusions

This study aimed to synthesize carbon nanotubes (CNTs) to remove CV dye from wastewaters. Three crucial variables studied in this research were contact time, initial concentration of dye solution, and pH of dye solution, respectively. The constant variables were the adsorbent dosage (1g), the temperature (room temperature), and the initial dye/ion solution of 10 mg/L for the isotherms. CNTs have demonstrated a good affinity for the removal of crystal violet dye. For maximum crystal violet adsorption, the process parameters were pH of 7, initial concentration of 10 mg/L, and contact time of 25 min, resulting in an 81.0% removal. This study's equilibrium data perfectly fits both the Langmuir and Freundlich isotherms. As for the reaction order, the

pseudo-first-order kinetic model was accurate. As a result of their particular features, carbon nanotubes showed great potential for use in wastewater treatment in removing CV dyes.

Conflict of interest: The authors declared no conflict of interest.

References

1. M. H. Dehghani, G. A. Omrani, R. R. Karri, Solid Waste—Sources, Toxicity, and Their Consequences to Human Health. In Soft Computing Techniques in Solid Waste and Wastewater Management, Elsevier, (2021), pp 205-213.
2. R. R. Karri, G. Ravindran, M. H. Dehghani, Wastewater—Sources, Toxicity, and Their Consequences to Human Health. In Soft Computing Techniques in Solid Waste and Wastewater Management, Elsevier, (2021), pp 3-33.
3. T. Aysu, and M. Küçük, Removal of crystal violet and methylene blue from aqueous solutions by activated carbon prepared from Ferula orientalis. International Journal of Environmental Science and Technology, 12 (2015), 2273-2284.
4. K. Zare, H. Sadegh, R. Shahryari-Ghoshekandi, B. Maazinejad, V. Ali, I. Tyagi, S. Agarwal, V. K. Gupta, Enhanced removal of toxic Congo red dye using multi walled carbon nanotubes: kinetic, equilibrium studies and its comparison with other adsorbents. J. Mol. Liq., 212 (2015), 266-271.
5. M. Chaudhary, R. Singh, I. Tyagi, J. Ahmed, S. Chaudhary, S. Kushwaha, Microporous activated carbon as adsorbent for the removal of noxious anthraquinone acid dyes: Role of adsorbate functionalization. J. Env. Chem. Eng., 9 (2021), 106308.
6. S. Kumar, G. Bhanjana, N. Dilbaghi, A. Umar, Multi walled carbon nanotubes as sorbent for removal of crystal violet. Journal of nanoscience and nanotechnology, 14 (2014), 7054-7059.
7. N. Mubarak, J. Sahu, E. Abdullah, N. Jayakumar, Removal of Heavy Metals from Wastewater Using Carbon Nanotubes. Separation & Purification Reviews, 43 (2014), 311-338.
8. M. Ruthiraan, N. M. Mubarak, R. K. Thines, E. C. Abdullah, J. N. Sahu, N. S. Jayakumar, P. Ganesan, Comparative kinetic study of functionalized carbon nanotubes and magnetic biochar for removal of Cd2+ ions from wastewater. Korean J. Chem. Eng., 32 (2015), 446-457.
9. N. M. Mubarak, J. N. Sahu, E. C. Abdullah, N. S. Jayakumar, P. Ganesan, Microwave assisted multiwall carbon nanotubes enhancing Cd(II) adsorption capacity in aqueous media. Journal of Industrial and Engineering Chemistry, 24 (2015), 24-33.
10. M. H. Dehghani, M. Mostofi, M. Alimohammadi, G. McKay, K. Yetilmezsoy, A. B. Albadarin, B. Heibati, M. AlGhouti, N. M. Mubarak, J. N. Sahu, High-performance removal of toxic phenol by single-walled and multi-walled carbon nanotubes: Kinetics, adsorption, mechanism and optimization studies. Journal of Industrial and Engineering Chemistry, 35 (2016), 63-74.
11. N. M. Mubarak, Y. T. Fo, H. S. Al-Salim, J. N. Sahu, E. C. Abdullah, S. Nizamuddin, N. S. Jayakumar, P. Ganesan, Removal of Methylene Blue and Orange-G from Waste Water Using Magnetic Biochar. Int. J. Nanosci., 14 (2015), 1550009.
12. F. S. A. Khan, N. M. Mubarak, Y. H. Tan, R. R. Karri, M. Khalid, R. Walvekar, E. C. Abdullah, S. A. Mazari, S. Nizamuddin, Magnetic nanoparticles incorporation into different substrates for dyes and heavy metals removal—A Review. Environ. Sci. Poll. Res., 27 (2020), 43526-43541.
13. F. S. A. Khan, N. M. Mubarak, Y. H. Tan, M. Khalid, R. R. Karri, R. Walvekar, E. C. Abdullah, S. Nizamuddin, S. A. Mazari, A comprehensive review on magnetic carbon nanotubes and carbon nanotube-based buckypaper for removal of heavy metals and dyes. Journal of Hazardous Materials, 413 (2021)

14. R. Kant, Textile dyeing industry an environmental hazard. Natural science, 4 (2012), 22.
15. M. R. Samarghandi, M. Zarrabi, A. Amrane, M. N. Sepehr, M. Noroozi, S. Namdari, A. Zarei, Kinetic of degradation of two azo dyes from aqueous solutions by zero iron powder: determination of the optimal conditions. Desalination Water Treat., 40 (2012), 137-143.
16. R. Khosravi, H. Eslami, A. Zarei, M. Heidari, A. N. Baghani, N. Safavi, A. Mokammel, M. Fazlzadeh, S. Adhami, Comparative evaluation of nitrate adsorption from aqueous solutions using green and red local montmorillonite adsorbents. Desalination Water Treat., 116 (2018)
17. B. Heibati, S. Rodriguez-Couto, N. G. Turan, O. Ozgonenel, A. B. Albadarin, M. Asif, I. Tyagi, S. Agarwal, V. K. Gupta, Removal of noxious dye—Acid Orange 7 from aqueous solution using natural pumice and Fe-coated pumice stone. J. Ind. Eng. Chem. , 31 (2015), 124-131.
18. N. D. Mu'azu, M. S. Manzar, M. Zubair, E. G. Alhajri, M. H. Essa, L. Meili, A. H. Khan, Volcanic ashe and its NaOH modified adsorbent for superb cationic dye uptake from water: Statistical evaluation, optimization, and mechanistic studies. Colloids and Surfaces A: Physicochemical and Engineering Aspects, 634 (2022), 127879.
19. M. S. Manzar, M. Zubair, N. A. Khan, A. Husain Khan, U. Baig, M. A. Aziz, N. I. Blaisi, H. I. M. Abdel-Magid, Adsorption behaviour of green coffee residues for decolourization of hazardous congo red and eriochrome black T dyes from aqueous solutions. Int. J. Environ. Anal. Chem., (2020), 1-17.
20. T. Madrakian, A. Afkhami, M. Ahmadi, H. Bagheri, Removal of some cationic dyes from aqueous solutions using magnetic-modified multi-walled carbon nanotubes. Journal of hazardous materials, 196 (2011), 109-114.
21. J.-L. Gong, B. Wang, G.-M. Zeng, C.-P. Yang, C.-G. Niu, Q.-Y. Niu, W.-J. Zhou, Y. Liang, Removal of cationic dyes from aqueous solution using magnetic multi-wall carbon nanotube nanocomposite as adsorbent. Journal of Hazardous Materials, 164 (2009), 1517-1522.
22. K. Zare, V. K. Gupta, O. Moradi, A. S. H. Makhlouf, M. Sillanpää, M. N. Nadagouda, H. Sadegh, R. Shahryari-Ghoshekandi, A. Pal, Z.-j. Wang, A comparative study on the basis of adsorption capacity between CNTs and activated carbon as adsorbents for removal of noxious synthetic dyes: a review. Journal of nanostructure in chemistry, 5 (2015), 227-236.
23. Z. Shahryari, A. S. Goharrizi, M. Azadi, Experimental study of methylene blue adsorption from aqueous solutions onto carbon nano tubes. (2010)
24. A. S. Sartape, P. D. Raut, S. S. Kolekar, Efficient adsorption of chromium (VI) ions from aqueous solution onto a low-cost adsorbent developed from limonia acidissima (wood apple) shell. Adsorption Science & Technology, 28 (2010), 547-560.
25. A. H. Khan, N. A. Khan, M. Zubair, M. Azfar Shaida, M. S. Manzar, A. Abutaleb, M. Naushad, J. Iqbal, Sustainable green nanoadsorbents for remediation of pharmaceuticals from water and wastewater: A critical review. Environ. Res., 204 (2022), 112243.
26. V. Sabna, S. G. Thampi, S. Chandrakaran, Adsorption of crystal violet onto functionalised multi-walled carbon nanotubes: Equilibrium and kinetic studies. Ecotoxicol. Environ. Saf., (2015)
27. M. H. Dehghani, M. Salari, R. R. Karri, F. Hamidi, R. Bahadori, Process modeling of municipal solid waste compost ash for reactive red 198 dye adsorption from wastewater using data driven approaches. Sci. Rep., 11 (2021)
28. Y. J. Lau, R. R. Karri, N. M. Mubarak, S. Y. Lau, H. B. Chua, M. Khalid, P. Jagadish, E. C. Abdullah, Removal of dye using peroxidase-immobilized Buckypaper/polyvinyl alcohol membrane in a multi-stage filtration column via RSM and ANFIS. Environ. Sci. Poll. Res., 27 (2020), 40121-40134.
29. N. Mubarak, J. Sahu, E. Abdullah, N. Jayakumar, P. J. D. Ganesan, R. Materials, Single stage production of carbon nanotubes using microwave technology. 48 (2014), 52-59.

30. F. S. A. Khan, N. M. Mubarak, M. Khalid, Y. H. Tan, E. C. Abdullah, M. E. Rahman, R. R. Karri, A comprehensive review on micropollutants removal using carbon nanotubes-based adsorbents and membranes. J. Env. Chem. Eng., 9 (2021)
31. F. S. A. Khan, N. M. Mubarak, M. Khalid, M. M. Khan, Y. H. Tan, R. Walvekar, E. C. Abdullah, R. R. Karri, M. E. Rahman, Comprehensive review on carbon nanotubes embedded in different metal and polymer matrix: fabrications and applications. Crit. Rev. Solid State Mater. Sci., (2021)
32. J. Liu, M. R. i Zubiri, B. Vigolo, M. Dossot, Y. Fort, J.-J. Ehrhardt, E. J. C. McRae, Efficient microwave-assisted radical functionalization of single-wall carbon nanotubes. 45 (2007), 885-891.
33. V. Sabna, S. G. Thampi, S. Chandrakaran, Adsorption of crystal violet onto functionalised multi-walled carbon nanotubes: Equilibrium and kinetic studies. Ecotoxicol. Environ. Saf., 134 (2016), 390-397.
34. I. A. Lawal, M. M. Lawal, M. A. Azeez, P. Ndungu, Theoretical and experimental adsorption studies of phenol and crystal violet dye on carbon nanotube functionalized with deep eutectic solvent. J. Mol. Liq., 288 (2019), 110895.
35. A. Ghosh, T. Basu, B. Manna, S. Bhattacharya, U. C. Ghosh, K. Biswas, Synthesis of a nanocomposite adsorbent with high adsorptive potential and its application for abatement of chromium (VI) from aqueous stream. Journal of Environmental Chemical Engineering, 3 (2015), 565-573.
36. N. Mubarak, J. Sahu, E. Abdullah, N. Jayakumar, P. Ganesan, Single stage production of carbon nanotubes using microwave technology. Diamond and Related Materials, 48 (2014), 52-59.
37. A. M. Aljeboree, A. F. Alkaim, A. H. J. D. Al-Dujaili, W. Treatment, Adsorption isotherm, kinetic modeling and thermodynamics of crystal violet dye on coconut husk-based activated carbon. 53 (2015), 3656-3667.
38. V. Gupta, and A. Nayak, Cadmium removal and recovery from aqueous solutions by novel adsorbents prepared from orange peel and Fe 2 O 3 nanoparticles. Chemical Engineering Journal, 180 (2012), 81-90.
39. K. Belay, and A. Hayelom, Removal of methyl orange from aqueous solutions using thermally treated egg shell (locally available and low cost biosorbent). (2014)
40. K. Elsherif, A. El-Dali, A. Alkarewi, A. Ewlad-Ahmed, A. Treban, Adsorption of crystal violet dye onto olive leaves powder: Equilibrium and kinetic studies. Chemistry International, 7 (2021), 79-89.
41. K. M. Elsherif, A. El-Hashani, I. Haider, Biosorption of Fe (III) onto coffee and tea powder: Equilibrium and kinetic study. Asian Journal of Green Chemistry, 2 (2018), 380-394.
42. V. K. Gupta, D. Pathania, N. Kothiyal, G. Sharma, Polyaniline zirconium (IV) silicophosphate nanocomposite for remediation of methylene blue dye from waste water. J. Mol. Liq., 190 (2014), 139-145.
43. K. Elsherif, I. Haider, A. El-Hashani, Adsorption of Co (II) ions from aqueous solution onto tea and coffee powder: equilibrium and kinetic studies. Journal of Fundamental and Applied Sciences, 11 (2019), 65-81.
44. M. A. M. Salleh, D. K. Mahmoud, W. A. W. A. Karim, A. J. D. Idris, Cationic and anionic dye adsorption by agricultural solid wastes: a comprehensive review. 280 (2011), 1-13.
45. C. Muthukumaran, V. M. Sivakumar, M. Thirumarimurugan, Adsorption isotherms and kinetic studies of crystal violet dye removal from aqueous solution using surfactant modified magnetic nanoadsorbent. Journal of the Taiwan Institute of Chemical Engineers, 63 (2016), 354-362.

46. M. Abbas, Z. Harrache, M. Trari, Removal of gentian violet in aqueous solution by activated carbon equilibrium, kinetics, and thermodynamic study. Adsorpt. Sci. Technol., 37 (2019), 566-589.
47. V. Sabna, S. G. Thampi, S. J. E. Chandrakaran, E. Safety, Adsorption of crystal violet onto functionalised multi-walled carbon nanotubes: equilibrium and kinetic studies. 134 (2016), 390-397.
48. S. Mohanty, S. Moulick, S. K. Maji, Adsorption/photodegradation of crystal violet (basic dye) from aqueous solution by hydrothermally synthesized titanate nanotube (TNT). Journal of Water Process Engineering, 37 (2020), 101428.
49. H. Shayesteh, A. Rahbar-Kelishami, R. J. D. Norouzbeigi, W. Treatment, Adsorption of malachite green and crystal violet cationic dyes from aqueous solution using pumice stone as a low-cost adsorbent: kinetic, equilibrium, and thermodynamic studies. 57 (2016), 12822-12831.
50. F. A. Pavan, E. S. Camacho, E. C. Lima, G. L. Dotto, V. T. Branco, S. L. Dias, Formosa papaya seed powder (FPSP): preparation, characterization and application as an alternative adsorbent for the removal of crystal violet from aqueous phase. J. Env. Chem. Eng., 2 (2014), 230-238.
51. A. Saeed, M. Sharif, M. Iqbal, Application potential of grapefruit peel as dye sorbent: kinetics, equilibrium and mechanism of crystal violet adsorption. Journal of hazardous materials, 179 (2010), 564-572.
52. A. S. Takabi, M. Shirani, A. Semnani, Apple stem as a high performance cellulose based biosorbent for low cost and eco-friendly adsorption of crystal violet from aqueous solutions using experimental design: Mechanism, kinetic and thermodynamics. Environmental Technology & Innovation, 24 (2021), 101947.
53. A. Ghazali, M. Shirani, A. Semnani, V. Zare-Shahabadi, M. Nekoeinia, Optimization of crystal violet adsorption onto Date palm leaves as a potent biosorbent from aqueous solutions using response surface methodology and ant colony. J. Env. Chem. Eng., 6 (2018), 3942-3950.
54. G. Vyavahare, P. Jadhav, J. Jadhav, R. Patil, C. Aware, D. Patil, A. Gophane, Y.-H. Yang, R. Gurav, Strategies for crystal violet dye sorption on biochar derived from mango leaves and evaluation of residual dye toxicity. J. Cleaner Prod., 207 (2019), 296-305.